의학박사 학위논문

신장 이식 거부반응에서 말초 혈액 단핵세포를 사용하여 차등 발현 유전자를 확인하기 위한 단일 세포 RNA 시퀀싱

Single Cell RNA Sequencing to Uncover Differential expression gene using Peripheral blood mononuclear cells according to Rejection type of Kidney allograft

울 산 대 학 교 대 학 원

의 학 과

임 성 준

신장 이식 거부반응에서 말초 혈액 단핵세포를 사용하여 차등 발현 유전자를 확인하기 위한 단일 세포 RNA 시퀀싱

지 도 교 수 신 성

이 논문을 의학박사 학위 논문으로 제출함

2024년 2월

울 산 대 학 교 대 학 원

의 학 과

임 성 준

임성준의 의학박사 학위 논문을 인준함

심사위원 황 상 현 인

심사위원 신 성 인

심사위원 권 현 욱 인

심사위원 권 준 교 인

심사위원 전 흥 만 인

울 산 대 학 교 대 학 원

2 0 2 4 년 2 월

ABSTRACT

Background

Analysis of immune pathways using peripheral blood-based gene expression patterns has been employed to elucidate the mechanism of rejection in kidney transplant recipients. Particularly, single-cell sequencing has enabled more precise research by confirming gene expression in specific cells. We aimed to identify differentially expressed genes (DEGs) associated with antibody-mediated rejection and T-cell-mediated rejection following kidney transplantation (KT).

Methods

A for-cause biopsy was performed on six KT recipients, who were categorized into three groups: no major abnormality (NOMOA), T cell-mediated rejection (TCMR), and antibody-mediated rejection (ABMR) according to the Revised Banff 2019 classification. Comprehensive single-cell sequencing analysis was performed using peripheral blood mononuclear cells (PBMCs) from these patients. The DEGs were confirmed using Gene Ontology (GO) biological pathway analysis.

Results

Out of a total of 52,766 cells, 33,185 cells were assessed, and poor-quality cells were excluded from the analysis. CD8+ terminally differentiated effector memory (Temra) T cells and NK T cells were highly abundant in the ABMR group. In CD8+ Temra T cells, 36 ABMR-specific genes were identified, with 20 DEGs involved in immune and inflammatory responses. STRING analysis using 20 genes showed that the most related genes were *LGALS1* and *ITM2A*, which are involved in plasma cell differentiation. There were 48 ABMR-specific genes in NK T cells, and 28 of them had significant functions in the GO biological pathway. Among these, the most relevant genes in the STRING analysis were *CD160* and *HLA-F*, which were confirmed to be involved in the positive regulation of NK cell degranulation. No

significant final cells and DEGs were identified in the TCMR group.

Conclusions

We investigated the distribution of PBMCs from KT recipients and identified DEGs in each cell. In the context of ABMR, *LGALS1* and *ITM2A* in CD8+ Temra T cells, and *CD160* and *HLA-F* in NK T cells, unequivocally play pivotal roles. The findings of this research will help identify transcripts suitable for future investigations into the mechanisms of ABMR and non-invasive diagnostic approaches.

TABLE OF CONTENTS

Abstract ····· i

Contents ····· iii

List of Tables and figures ····· iv

1. Introduction ····· 1

2. Materials and Methods ····· 2

A. Patient selection ····· 2

B. Sample processing and microfluidic single-cell sequencing ····· 3

C. Quality control and filtering ····· 5

D. Cell clustering and cell type annotation ····· 5

E. DEGs analysis and finding specific DEGs by Venn diagram ····· 6

F. Identification of meaningful DEGs using a two-track strategy ····· 6

3. Results ····· 7

A. Patient characteristics and histopathology ····· 7

B. PBMCs and T cell subset clustering and transcriptome characteristics ····· 10

C. Second annotation for a more specific subtype designation of each cell····· 10

D. Finding ABMR and TCMR specific DEGs ····· 14

E. Finding meaningful DEGs in CD8+ Temra T cell and NK T cell ··· 14

4. Discussion ····· 17

5. References ····· 20

6. Supplementary data ····· 22

국문요약 ····· 30

List of Tables

Table 1. Baseline characteristics according to pathologic diagnosis ····· 7

List of Figures

Figure 1. Schematic diagram of the overall design of the research ····· 4

Figure 2. PBMCs and T cell subset clustering and transcriptome characteristics ····· 9

Figure 3. CD8+ T cell subset clustering ····· 11

Figure 4. NK cell subset clustering ····· 12

Figure 5. Finding ABMR and TCMR specific DEGs ····· 13

Figure 6. ABMR associated meaningful DEGs in CD8+ Temra T cell ····· 15

Figure 7. ABMR associated meaningful DEGs in NK T cell ····· 16

List of Supplementary Tables

Supplementary table 1. Cell and subtype cell marker for annotation ··· 22

Supplementary table 2. Pathologic findings according to the Revised Banff 2019 classification ····· 23

Supplementary table 3. Proportions of different cell types ····· 23

Supplementary table 4. Proportions of different subset cell types ····· 24

Supplementary table 5. Meaningful DEGs associated ABMR in each subtype cells ····· 25

List of Supplementary figures

Supplementary figure 1. Quality control and filtering ····· 26

Supplementary figure 2. T cell subset marker and quality control ····· 27

Supplementary figure 3. Second annotation of CD4+ T cells, B cells, and Myeloid cells ····· 28

Supplementary figure 4. ABMR-specific DEGs and meaningful DEGs in IL1β+ monocyte ····· 29

1. **Introduction**

Kidney transplantation (KT) is the most effective treatment for end-stage renal disease[1]. However, rejection remains a critical problem that can deteriorate graft function and threaten the survival of both the graft and recipients[2,3]. The traditional diagnostic approaches for kidney transplant rejection are serologic evaluation of donor-specific antibodies (DSAs) and graft biopsy. However, graft biopsy has several limitations, including invasiveness, risk of complications, and the need for histological interpretation[4,5]. Additionally, laboratory tests for DSAs provide limited insights into the underlying immunological mechanisms and the existence of immunological memory, as antibodies represent the final products of the immune response to alloantigen[6]. For these reasons, the discovery and application of non-invasive molecular markers for the effective diagnosis of renal transplant rejection have been studied extensively, particularly transcriptomics in peripheral blood[7-10].

The utilization of single-cell genomics technologies has brought about a paradigm shift in our understanding of the immune system. Single-cell transcriptomics technologies provide a comprehensive assessment of the transcriptional profiles of immune cells. They have been successfully used to discover novel immune cell subtypes, identify gene modules that govern immune reactions, and investigate the diversity of lymphocyte antigen receptors[11]. The technique enables researchers to examine the diverse makeup of immune cells in peripheral blood mononuclear cells (PBMCs), offering insights into the functions of T cells, B cells, NK cells, and other immune cell populations[10,12].

Although the proportion and absolute number in PMBCs are small, NK cells play a role in antibody-mediated rejection (ABMR)[13], an increase in CD56-positive NK cells has been reported in T-cell-mediated rejection (TCMR) biopsies[14]. Similarly, myeloid cells, despite their smaller numbers compared to lymphocytes, play a crucial role in modulating both innate and adaptive immune reactions. After

transplantation, myeloid cells have two contrasting functions. Firstly, they trigger the immune response by stimulating the activation and proliferation of effector T-cells. Secondly, they counter-regulate inflammation, uphold tissue homeostasis, and promote tolerance[15].

In a previous study, differential expression genes (DEGs) for chronic active ABMR were reported through single-cell RNA sequencing on PBMCs[10]. However, the study did not compare ABMR and TCMR, and only analyzed the DEGs of T and B lymphocytes. Furthermore, there was no analysis of DEGs in NK cells or myeloid cells, which are also crucial in immune responses. Therefore, in this study, we aimed to identify significant DEGs among control, TCMR, and ABMR after KT by conducting single-cell RNA sequencing using PBMCs. Overall PBMCs were analyzed, including previously attempted T lymphocytes, B lymphocytes, NK cells, and monocytes. The biological functions of the identified DEGs were confirmed.

2. **Materials and Methods**

A. Patient selection

Six peripheral blood samples were obtained from kidney transplant recipients at Asan Medical Center for this study. All patients provided written informed consent, and the institutional review board and ethics committee approved the study (AMC IRB number, 2021-0284). The surgeries were performed between July 2012 and October 2021. Between October 2021 and November 2022, we performed biopsies based on clinical needs and collected peripheral blood for research when patients were hospitalized for biopsies. The time difference between surgery and blood collection varied from 1 to 113 months (**Table 1**). We followed the established protocol and used an 18-gauge biopsy gun to collect needle-core biopsies. The renal histopathological examination was conducted in a double-blind

manner by two observers, following the Revised Banff 2019 classification[4]. The allograft histopathology was classified into three groups: no major abnormality (NOMOA) group (n=2), TCMR group (n=2), and ABMR group (n=2). The NOMOA group exhibited no evidence of active rejection. The TCMR group was diagnosed with chronic active TCMR, as indicated by a Banff lesion score of *ti* ≥ 2 and a Banff lesion score of *i-IFTA* ≥ 2. Other known causes of *i-IFTA*, such as pyelonephritis or BK-virus nephritis, were ruled out and the Banff lesion score of *t* was also ≥ 2. The ABMR group was diagnosed with active ABMR, meeting at least one criterion for AMR activity and at least one criterion for antibody interaction with tissue, as well as at least one criterion for DSA or equivalent[4].

B. Sample processing and microfluidic single-cell sequencing

The overall procedures of the study are summarized in **Figure 1**. The specimens were centrifuged at 400 x g for 5 minutes at 4°C and the supernatant was removed. To isolate PBMCs, red blood cell lysate (SolarBio, R1010, China) was added and left on ice for 15 minutes. This was followed by another centrifugation at 400 x g at 4°C for 10 minutes. The supernatant was then discarded, and the PBMCs were resuspended in phosphate-buffered saline to create a single-cell suspension. Single-cell suspensions containing 1×10^5 cells/mL in PBS (HyClone) were prepared.

The cells were loaded onto microfluidic devices, and the scRNA-seq libraries were generated using the Chromium Next GEM Single Cell 3′ Kit v2 (Dual Index) on the Chromium platform, provided by 10x Genomics in the USA. The library preparation process followed the guidelines provided by the manufacturer. The quality of the cDNA library was assessed using an Agilent Bioanalyzer from Agilent in the USA. Subsequently, individual libraries were diluted to 4 nM and then pooled for sequencing. The scRNA libraries were sequenced using the Illumina NovaSeq

6000 platform.

Figure 1. Schematic diagram of the overall design of the research

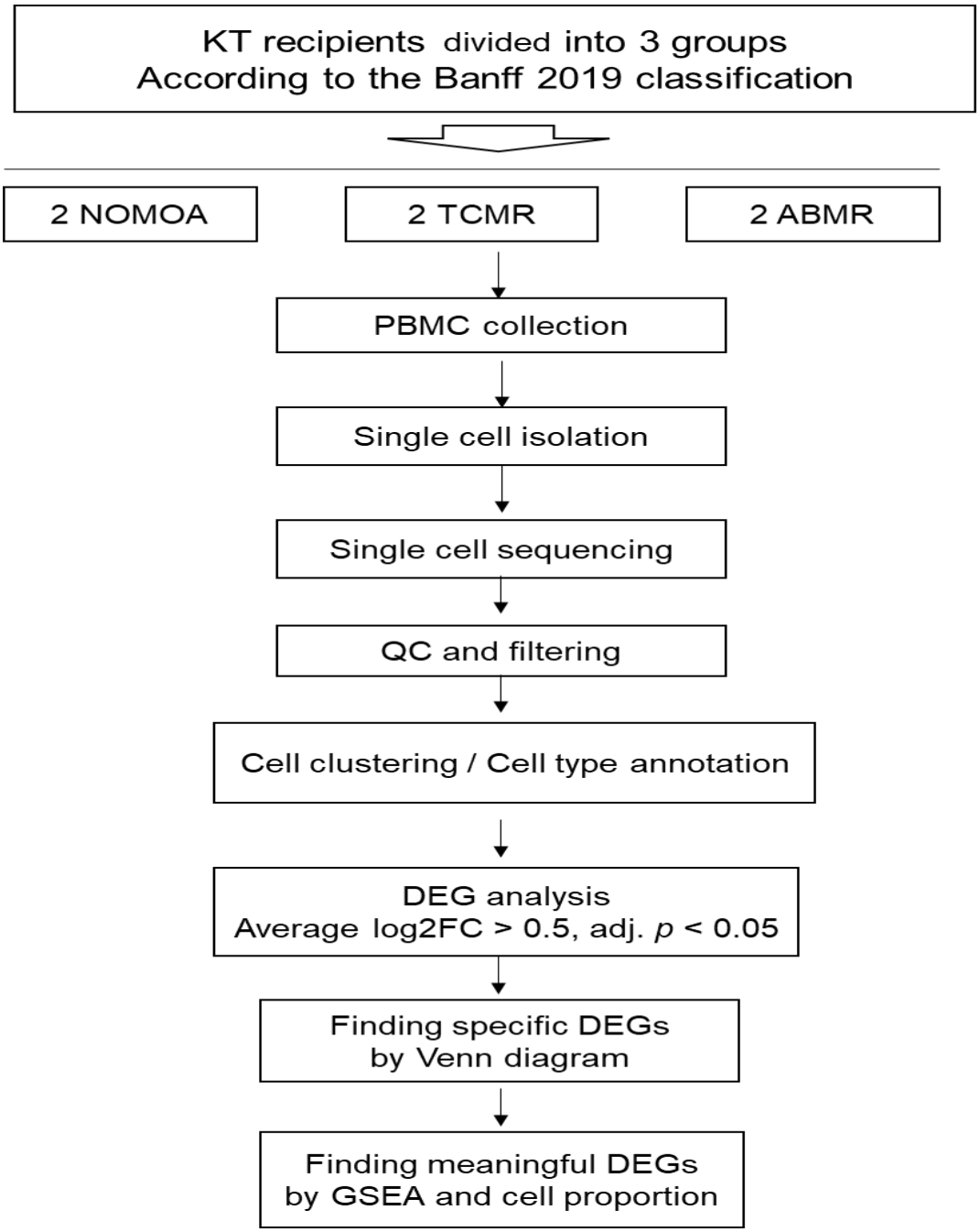

C. Quality control and filtering

The FASTQ sequencing reads underwent processing using Cell Ranger version 7.1.0 (provided by 10x Genomics) for alignment to the GRCh38 human transcriptome reference. Subsequently, data preprocessing was carried out using Seurat v4.3.0, applying quality control criteria to eliminate cells that exhibited a high percentage of mitochondrial genes using the miQC R package, as well as those with an RBC marker gene percentage less than 5% and a low number of expressed RNA features (<500). The results of cell isolation and quality control are shown in **Supplement Figure 1**. A total of 52,766 cells were isolated, and cells with an intracellular mitochondrial gene ratio of more than 20% were excluded due to apoptosis or unhealthy status. Additionally, cells with an intracellular RNA count of less than 500 were excluded for the same reason. Doublets that could not be isolated as single cells by oil particles were excluded. When excluding cells for duplicate reasons, a total of 19,581 cells were excluded, and 33,185 cells were analyzed.

D. Cell clustering and cell type annotation

Following the quality check, the raw count data was normalized and scaled. Principal component analysis (PCA) was performed using Seurat, focusing on the 2,000 most variable features. After using Harmony version 1.0.3 for batch effect correction, we included the top 30 calculated dimensions in the dimension reduction process to create a Uniform Manifold Approximation and Projection (UMAP). Then, we applied the Louvain algorithm to identify clusters. To identify cell types, we used a combination of unsupervised clustering and differential expression analysis. For the first annotation, manual annotation was performed by comparing the top differentially expressed genes with the cell type-specific expression patterns documented in previous reports (**Supplement Table 1**). The

second annotation for each cell subtype was carried out using the FindClusters function in Seurat, followed by manual annotation for similar clusters.

E. DEGs analysis and finding specific DEGs by Venn diagram

For each cell subtype, DEG testing was performed using the FindMarkers function in the Seurat R package. DEGs were filtered using a minimum log fold change of 0.5 and an adjusted p value of < 0.05. A Venn diagram was created to compare the up-regulated genes in the NOMOA, TCMR, and ABMR groups (Draw Venn Diagram (ugent.be)). Genes from distinct regions without overlap were defined as differentially expressed genes specific to ABMR and TCMR.

F. Identification of meaningful DEGs using a two-track strategy

Gene set enrichment analysis (GSEA) was conducted using the genekitr package with ABMR- and TCMR-specific DEGs from each cell type, based on Gene Ontology (GO) terms and Kyoto Encyclopedia of Genes and Genomes (KEGG) pathways. A two-track strategy was used to identify significant cells and genes from a large pool of subtype cells and their numerous DEGs. First, as an essential criterion, only the pathways related to inflammatory and immune responses were restricted to a p-value < 0.01 in the GSEA results. The genes involved in these pathways were identified as ABMR-meaningful DEGs and TCMR-meaningful DEGs. As a second condition, cells with a cell ratio exceeding 30% compared to other groups were defined as cells with a significant distribution. We considered the first criterion essential and selected the final meaningful cells and DEGs by referring to the second condition. Afterwards, STRING analysis (STRING: functional protein association networks (string-db.org)) was performed to identify the most significant genes.

3. **Results**

A. Patient characteristics and histopathology

We divided the patients into three groups, each consisting of two patients, according to the revised 2019 Banff classification. The NOMOA group is patients with no evidence of active rejection on histopathology. The TCMR group included patients diagnosed with chronic active TCMR, while the ABMR group included patients diagnosed with active ABMR. The histopathological findings of these patients are summarized in **Supplementary Table 2**. The preoperative clinical information and biopsy results for each group are summarized in **Table 1**. The patients' ages range from 42 to 61 years. The NOMOA 2 patient underwent a second kidney transplant, which was ABO-incompatible (ABOi). One of the patients in the TCMR group had a positive flow cytometry crossmatch, so transplantation was performed after rituximab and plasmapheresis. All maintenance immunosuppressants were initially started with tacrolimus, but the TCMR group switched to cyclosporine due to drug side effects, including hair loss and diabetes. Three patients had DSA before surgery. For patients with re-transplanted NOMOA, an indication biopsy was performed one month after surgery due to the development of de novo DSA. Basal creatinine averaged 1.13 mg/dL, and the creatinine level at the time of biopsy was 1.43 mg/dL, indicating a creatinine increase of 26.5%. At the time of biopsy, there were a total of 5 patients with DSA, with 4 patients in both the TCMR group and ABMR group having de novo DSA. No patient was diagnosed with a urinary tract infection before or after the biopsy.

Table 1. Baseline characteristics according to pathologic diagnosis

	NOMOA1	NOMOA2	TCMR1	TCMR2	ABMR1	ABMR2
Age	50	42	52	61	56	51

Sex	M	F	M	F	F	F
BMI, kg/m^2	21.1	20.4	21.8	20.3	23.6	25.1
2nd transplantation (Y/N)	N	Y	N	N	N	N
ABOi (Y/N)	N	Y	N	N	N	Y
Deceased donor (Y/N)	N	N	N	N	Y	N
Crossmatching positive (Y/N)	N	N	N	Y	N	N
HLA mismatching	2	1	5	3	1	4
Induction						
Simulect	Y	Y	Y	Y	N	Y
Thymoglobuline	N	N	N	N	Y	N
Immunosuppressants						
Tacrolimus	Y	Y	N	N	Y	Y
Cyclosporine	N	N	Y	Y	N	N
Steroid	Y	Y	Y	Y	Y	Y
PRA I_pre op (%)	-	30	0	29	84	1
PRA II_pre op (%)	-	88	0	62	62	8
DSA_pre op (Y/N)	-	Y	N	Y	Y	N
Op to Biopsy (month)	113	1	6	24	44	59
Basal SCr (mg/dl)	1.32	1.00	1.33	0.86	0.95	1.32
SCr at biopsy (mg/dl)	1.64	1.00	2.0	1.01	1.32	1.61
SCr elevation (%)	24	0	50	17	39	22
PRA I at biopsy (%)	4	29	75	0	81	4
PRA II at biopsy (%)	4	67	93	98	90	66
DSA at biopsy (Y/N)	N	Y	Y	Y	Y	Y
Denovo_DSA at biopsy (Y/N)	N	N	Y	Y	Y	Y
UA_alb	0	0	0	0	0	0
UA_Nit	0	0	0	0	0	1
UA_WBC	0	0	0	0	0	0

Abbreviations: NOMOA, no major abnormalities; BMI, body mass index; ABOi, ABO incompatible; PRA, panel reactive antibody; DSA, donor-specific antibody; pre-op, preoperative; SCr, serum creatinine; UA, urinalysis

Figure 2. PBMCs and T cell subset clustering and transcriptome characteristics

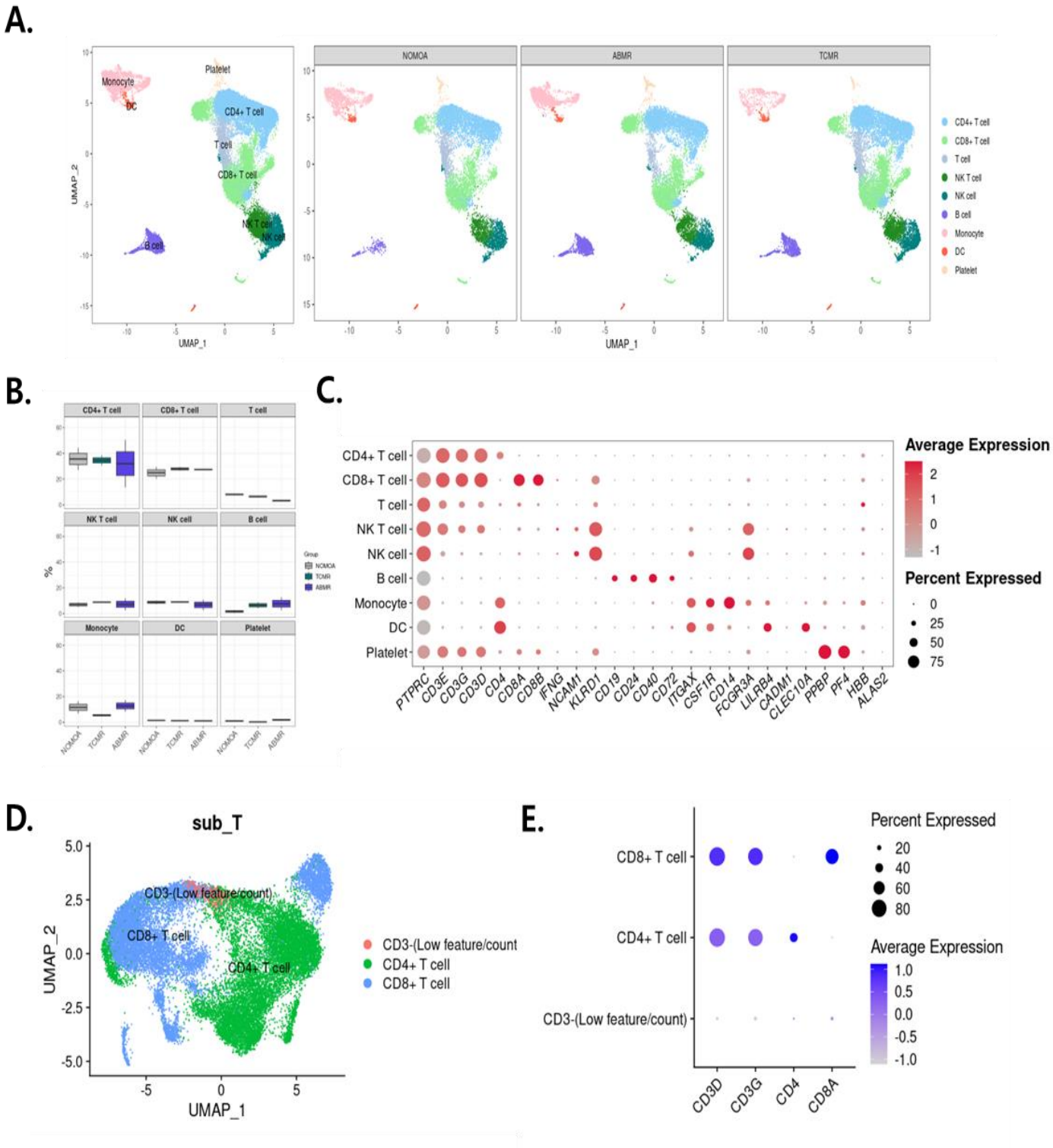

B. PBMCs and T cell subset clustering and transcriptome characteristics

Single-cell RNA sequencing analysis was performed as previously described, and a total of 33,185 PBMCs were identified (NOMOA group, 9501 [28.6%]; ABMR group, 11918 [35.9%]; TCMR group, 11766 [35.4%]). All cells were identified using the markers listed in **Supplementary Table 1** and visualized using cell projection clustering (UMAP). These cell clusters include CD4+ T cells, CD8+ T cells, T cells, natural killer T (NK T) cells, NK cells, B cells, monocytes, dendritic cells (DC), and platelets. **Figure 2B** and **Supplementary Table 3** show the number and proportion of cells in the three groups. In all groups, CD4+ T cells and CD8+ T cells were the most abundant cell types. B cells were relatively more abundant in the ABMR and TCMR groups (NOMOA group 1.8%, TCMR group 6.7%, ABMR group 8.1%), and monocytes were more prevalent in the ABMR group compared to the TCMR group (TCMR group 5.4%, ABMR group 13.2%). **Figure 2C** shows the distribution of characteristic marker genes for these 9 cell clusters. Thus, we confirmed the cell clusters and composition among the three groups.

Re-clustering was performed on the T cells that were most prominent. Out of a total of 21,853 cells (**Figure 2D**), 510 CD3- cells were excluded due to their low feature and high mitochondrial gene representation. The subsequent analysis was then conducted with the remaining T cells. The distribution of markers in **Figure 2E** is presented in **Supplementary Figure 2A**, and T cell quality control is shown in **Supplementary Figure 2B**.

C. Second annotation for a more specific subtype designation of each cell

Clusters for CD8+ T cells, CD4+ T cells, NK cells, B cells, and myeloid cells identified in the initial annotation process were determined using the FindClusters function in Seurat. Subsequently, a second annotation was carried out using

markers associated with previously known cell subtypes. The markers used in the second annotation for each cluster are also listed in **Supplementary Table 1**.

Figure 3. CD8+ T cell subset clustering

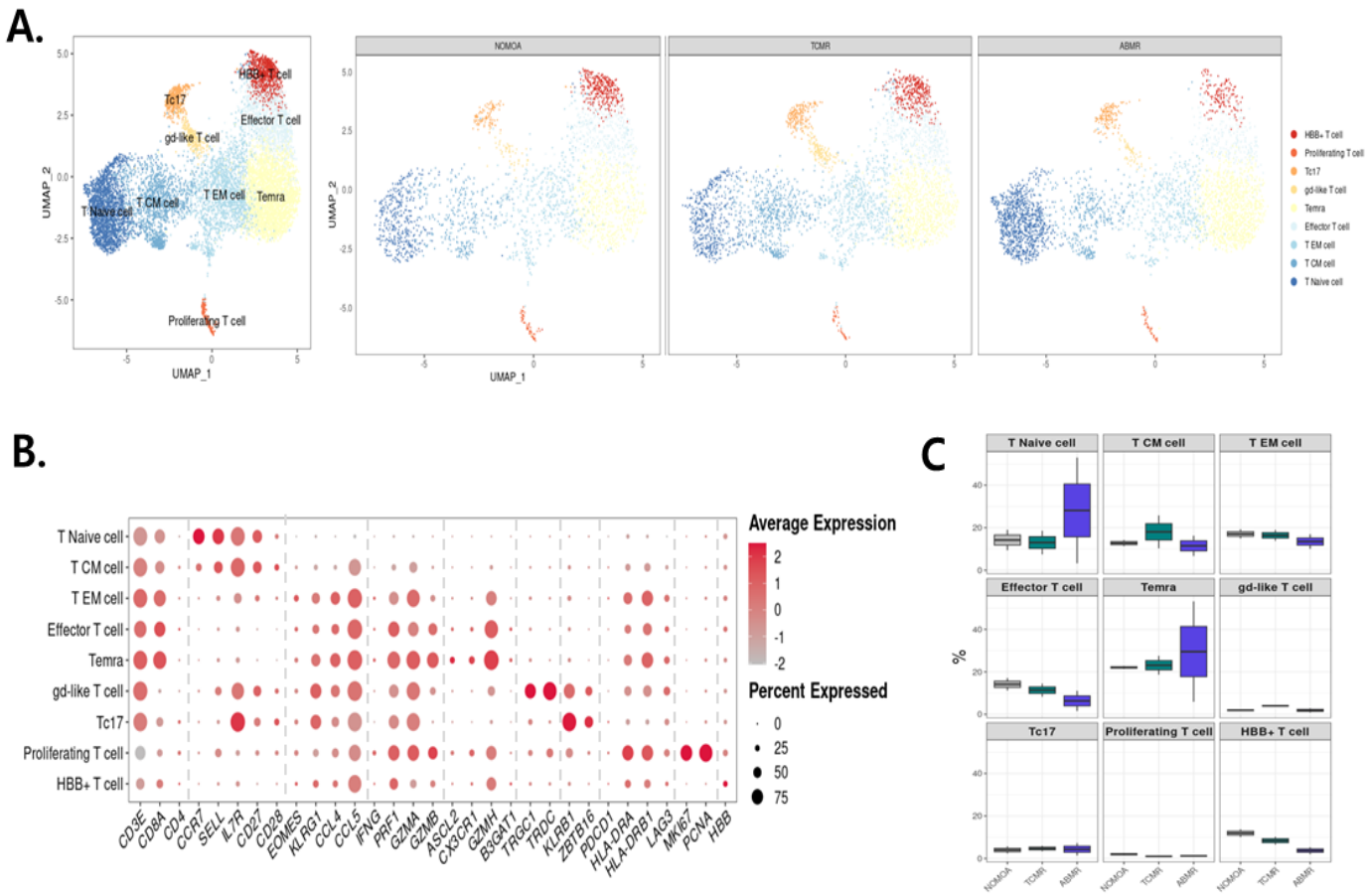

CD8+ T cells were divided into nine subsets, and their distribution depicted using UMAP is illustrated in **Figure 3A**. The markers used are highlighted in **Figure 3B**. Upon examining the variations in cell distribution among NOMOA, TCMR, and ABMR groups, we found that T naïve cells and Terminally Differentiated Effector Memory (Temra) cells are more prevalent in the ABMR group compared to the other two cohorts. Examining the critical markers that validate the clusters, T naïve

cells expressed CCR7, SELL+++, and IL7R+, while Temra T cells exhibited ASCL2, CX3CR1+, GZMH+, CD27, and CD28-. Subsequently, NK cells were classified into distinct groups: NK T cells expressing CD3, CD56 bright NK cells expressing NCAM1 (CD56) and GZMK, and CD56 dim NK cells expressing FCGR3A (CD16) (**Figure 4A**, **4B**). While the distribution seemed similar for each group, there was a higher prevalence of NK T cells in the ABMR group compared to the other two groups. A similar analysis was performed on CD4+ T cells, B cells, and myeloid cells, and the results are depicted in **Supplementary Figure 3**.

Figure 4. NK cell subset clustering

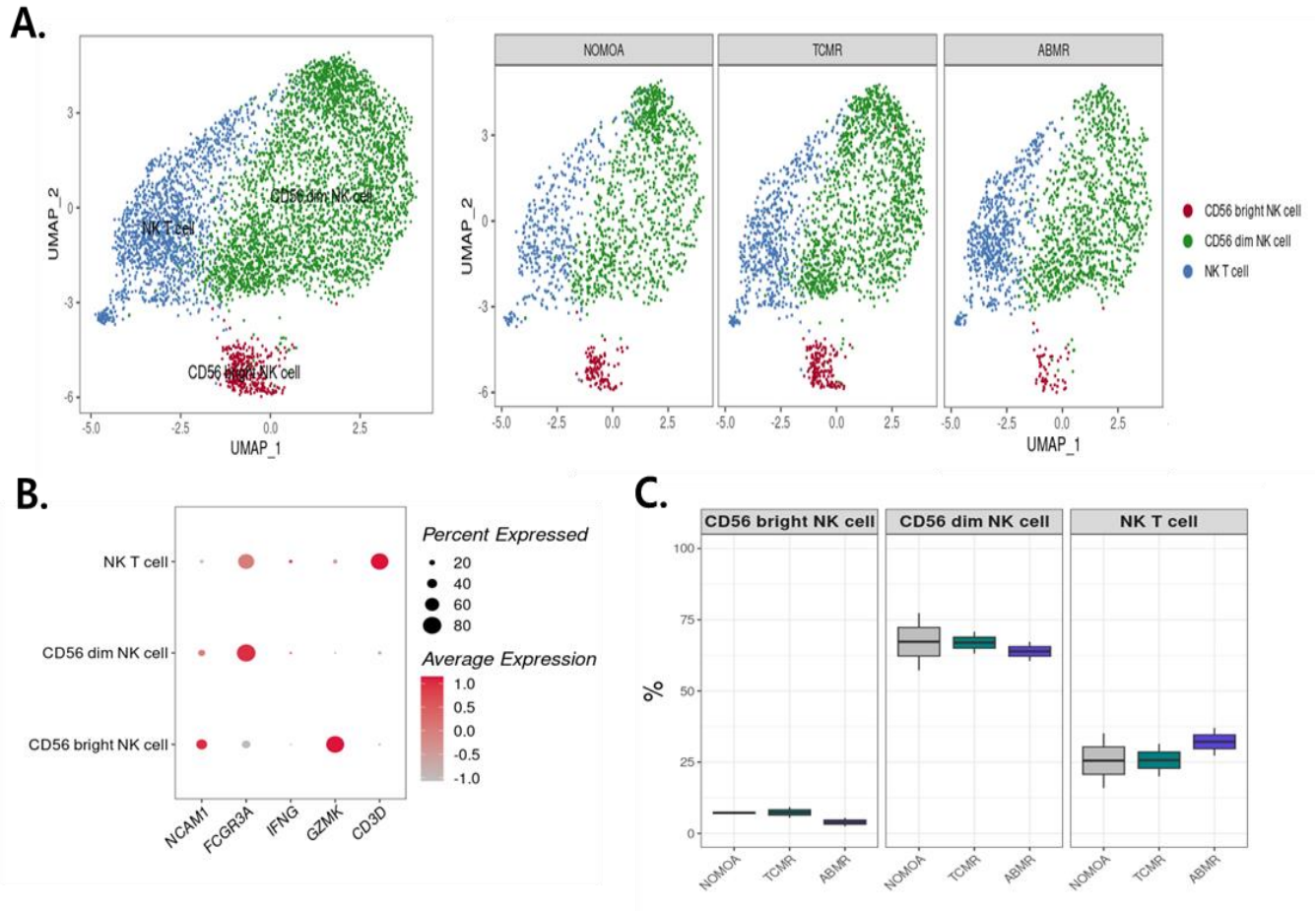

Figure 5. Identification of ABMR- and TCMR-specific DEGs

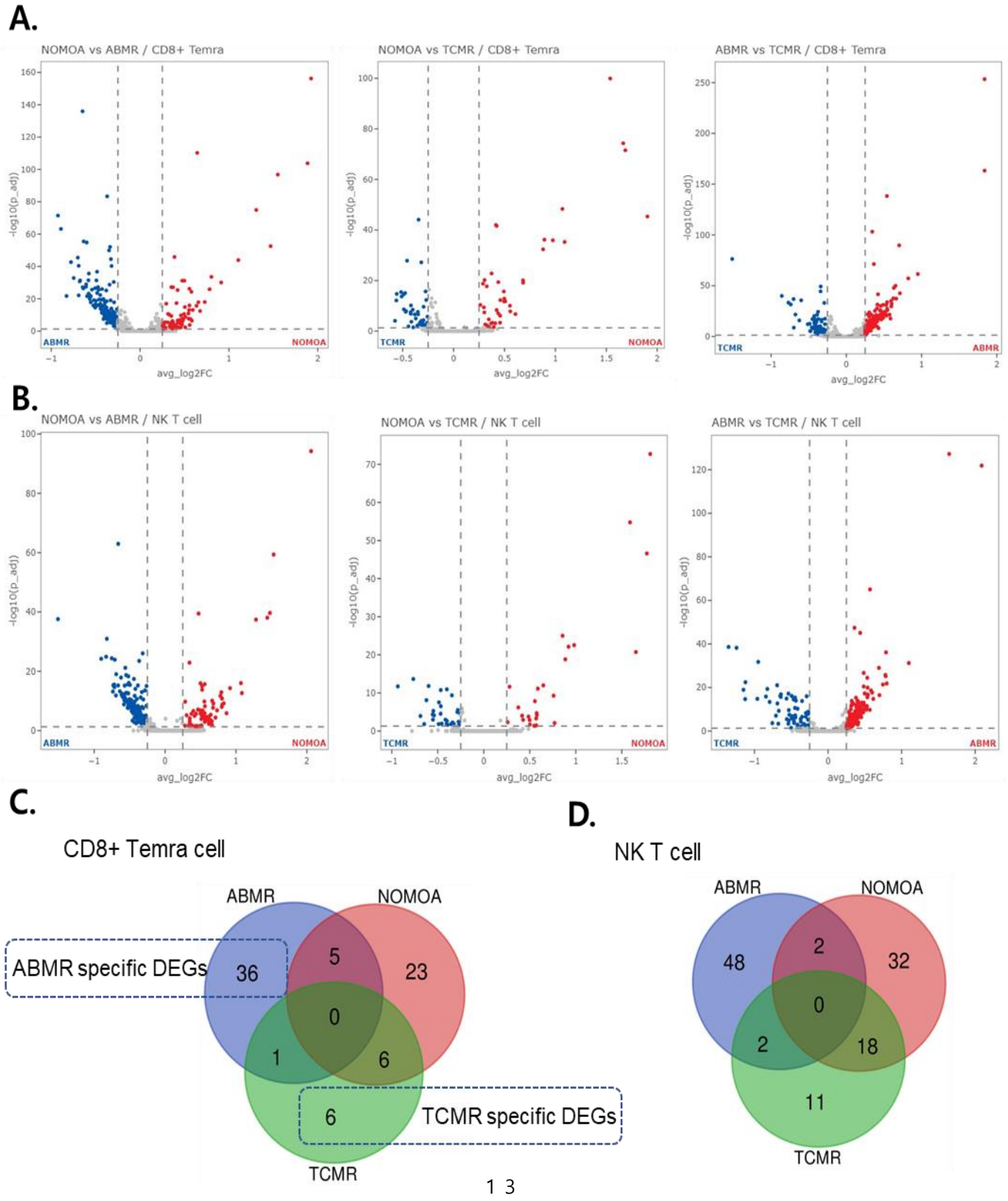

D. Identification of ABMR- and TCMR-specific DEGs

We identified DEGs for the NOMOA vs. ABMR, NOMOA vs. TCMR, and ABMR vs. TCMR for each subgroup of cells using the FindMarkers function in the Seurat R package. Within the outcomes for 32 subclusters, **Figures 5A** and **5B** illustrate the findings for CD8+ Temra T cells and NK cells. The number of DEGs between NOMOA vs. ABMR, NOMOA vs. TCMR, and ABMR vs. TCMR in CD8+ Temra T cells was 5095, 4641, and 5164, respectively. Among the identified DEGs, the up-regulated DEGs in each group that showed a log fold change of 0.5 or higher and an adjusted p value of < 0.05 were as follows: 42 for ABMR, 34 for NOMOA, and 13 for TCMR. A Venn diagram was created using these values. At this time, 36 genes uniquely belonging to the ABMR region were identified as ABMR-specific DEGs of CD8+ Temra T cells, and 6 genes uniquely belonging to the green region were identified as TCMR-specific DEGs of CD8+ Temra T cells (**Figure 5C**). Analysis of NK T cells was also performed in the same process, and 48 ABMR-specific DEGs of NK T cells were identified.

E. Finding meaningful DEGs in CD8+ Temra cells and NK T cells

In line with the original objectives of the study, GO biological process analysis was performed using ABMR-specific DEGs and TCMR-specific DEGs from each cell to identify genes associated with rejection and inflammatory responses. In the results of the GO biological process analysis, pathways that met the significance threshold of a p value < 0.01 were considered significant. It was confirmed that ABMR-specific DEGs in CD8+ Temra T cells participated in multiple pathways related to rejection and inflammatory responses (**Figure 6B**). The most significant pathways included the adaptive immune response (GO:0002250), cellular response to interferon-gamma (GO:0071346), and immune response (GO:0006955). ABMR-specific DEGs involved in rejection and inflammatory response pathways were

defined as ABMR-associated meaningful DEGs, while genes involved in unrelated pathways such as positive wound healing (GO:0090303) were excluded. Among the 36 ABMR-specific DEGs in CD8+ Temra T cells, 20 genes were involved in significant pathways (**Supplementary Table 5**).

Figure 6. ABMR-associated meaningful DEGs in CD8+ Temra T cells

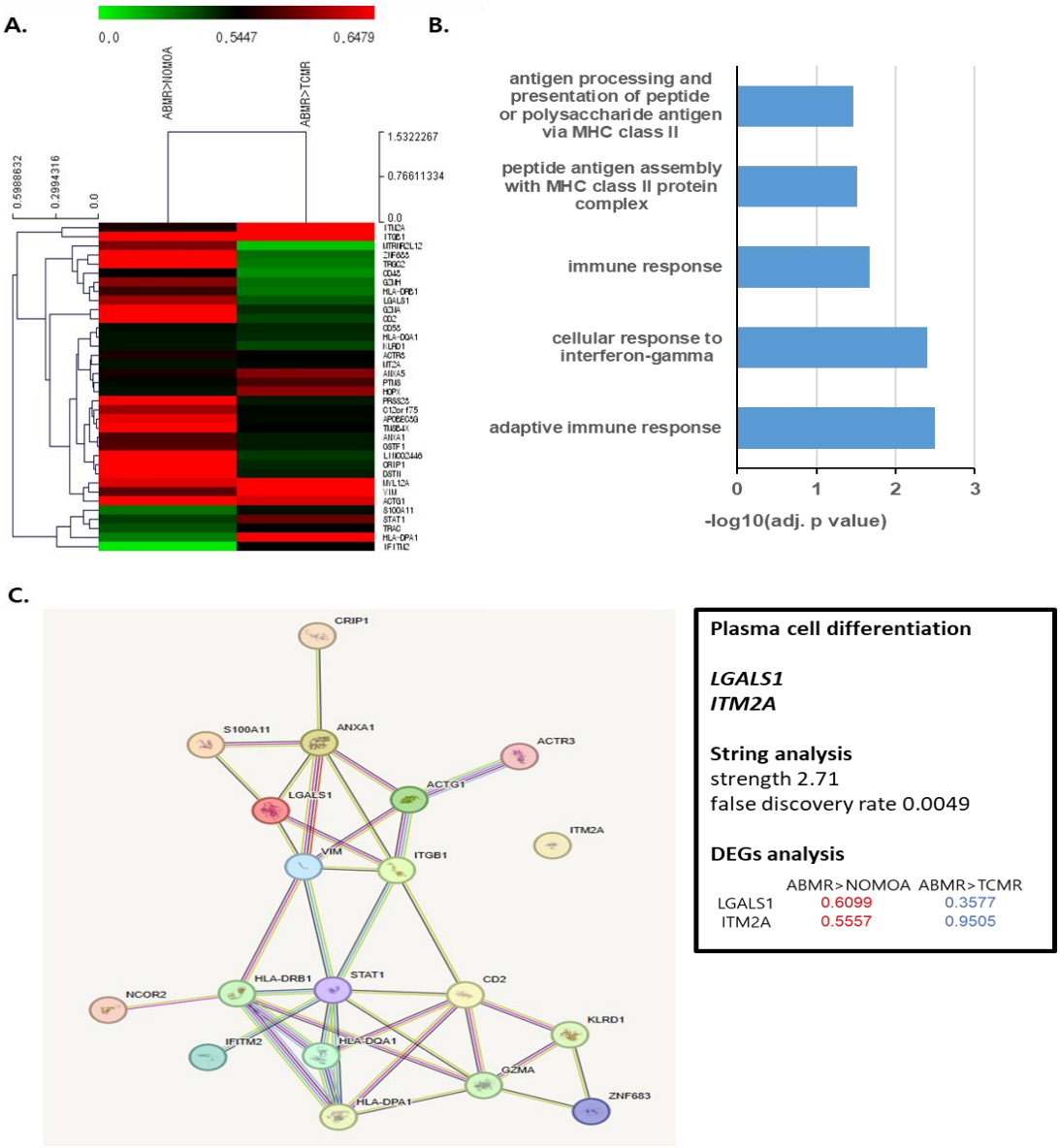

The analysis was conducted across all 32 subgroup cells, and cells were considered meaningful if the GSEA results for the identified DEGs were strongly associated with rejection or inflammatory response. Alternatively, cells with a cell count exceeding 30% compared to other groups were also included in the final selection. Unfortunately, in TCMR, while GSEA was significant, there were no cells distributed in greater numbers than other groups. In ABMR, the GSEA results were also significant, showing that CD8+ Temra T cells and NK T cells were distributed more than 30% higher than in the other two groups. The composition ratio of each cell subset is presented in **Supplementary Table 4**.

Figure 7. ABMR-associated meaningful DEGs in NK T cells

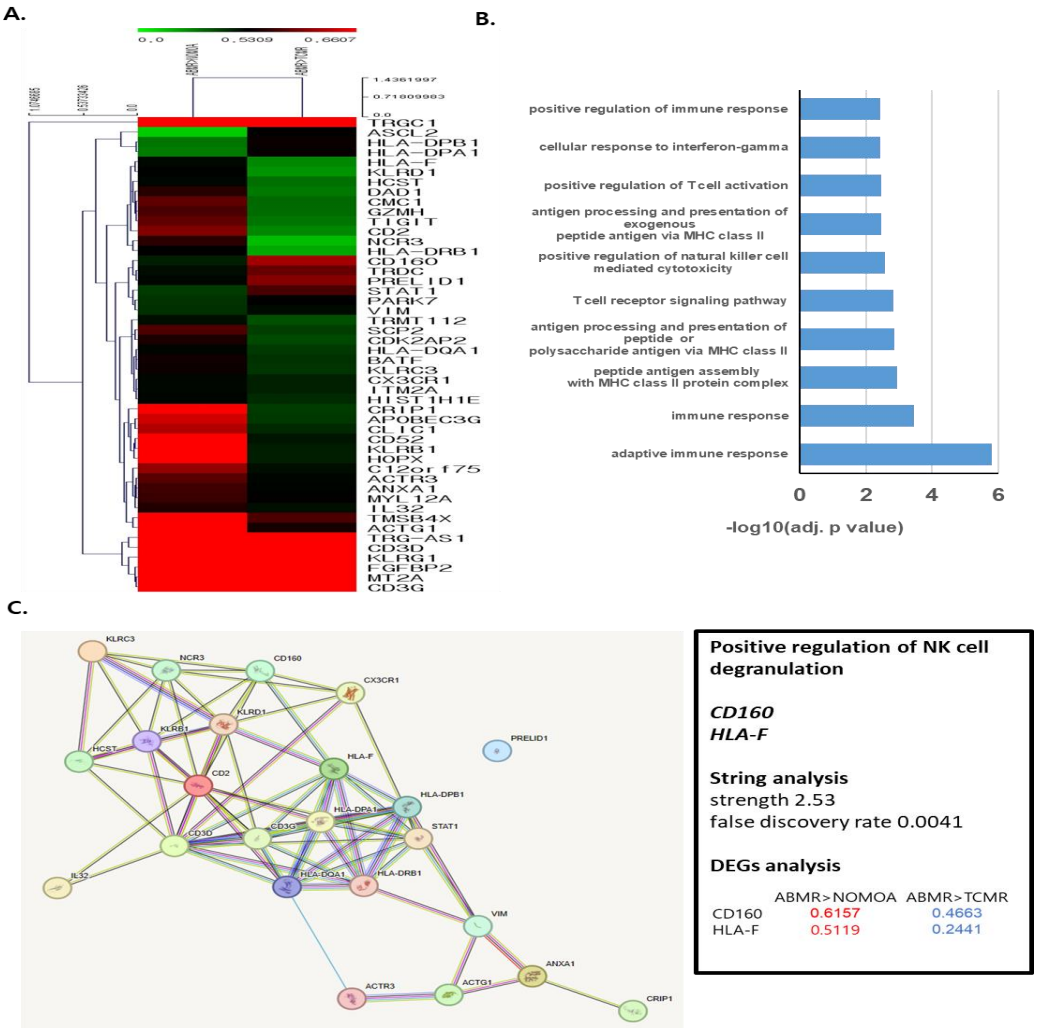

STRING analysis was conducted to identify the most meaningful DEGs among the 20 ABMR-associated meaningful DEGs in CD8+ Temra T cells (**Figure 6C**). Several genes appeared to be related to each other, and the genes that showed the strongest connection were *LGALS1* and *ITM2A*, which are involved in plasma cell differentiation, with a strength of 2.71 and a false discovery rate of 0.0049. The log2FC values of *LGALS1* and *ITM2A* were 0.6099 and 0.5557 in ABMR vs NOMOA and ABMR vs TCMR, respectively. Both genes were approximately 1.5 times more abundant than other groups.

The GSEA results of ABMR-specific genes in NK T cells are shown in **Figure 7B**. ABMR-specific genes of NK T cells were also confirmed to be involved in various immune and inflammatory responses, and the most strongly related pathways were the adaptive immune response (GO:0002250) and immune response (GO:0006955). Similarly, only genes involved in immune and inflammatory responses were classified as meaningful genes, leading to the identification of a total of 28 significant genes after excluding duplicates. Among these, STRING analysis was performed to identify the most meaningful genes, which showed that *CD160* and *HLA-F* were involved in the positive regulation of NK cell degranulation, with a strength of 2.53 and a false discovery rate of 0.0041. The two genes were also present approximately 1.5 times more frequently than the other two groups, with log2FC values of 0.6157 and 0.5119, respectively.

4. **Discussion**

In this study, we categorized KT recipients into three groups—NOMOA, TCMR, and ABMR—according to histopathologic findings from patients who underwent a for-cause biopsy. Subsequently, single-cell sequencing was conducted using their PBMCs. Various cells within PBMCs were divided into a total of 32 clusters, and DEGs between groups were identified for each cell. Among them, cells in which

GSEA was strongly associated with immune or inflammatory responses and had a distribution that was 30% more than other groups were defined as the final meaningful cells and meaningful DEGs. Finally, string analysis was used to identify the most meaningful DEGs, and *LGALS1* and *ITM2A* were found to be involved in ABMR in CD8+ Temra T cells, while *CD160* and *HLA-F* were identified as genes involved in ABMR in NK T cells. No cells or genes meeting the conditions were identified in the TCMR group.

The significant presence of CD8+ Temra T cells and their association with ABMR has been previously documented[16,17]. Furthermore, while there have been no reports of kidney transplant rejection, *LGALS1* was confirmed in the mouse corneal allograft rejection model using single-cell RNA sequencing[18]. Concurrently, the mRNA level of *ITM2A* was shown to be particularly high in the urine of patients who experienced acute rejection after KT[19]. Lastly, although it did not affect the survival of the graft, a study reported a delay in T cell division in *CD160* knockout mice compared to the wild type[20].

Although IL1β+ monocytes were relatively less abundant in the ABMR group compared to other groups, the GSEA results showed significance. ABMR-specific DEGs satisfying Log2FC > 0.5 and p-value < 0.05 were most abundant, totaling 205. The most significant DEGs involved in rejection and inflammatory reactions were also the largest, at 58. STRING analysis using these 58 genes is shown in Supplementary Figure 4E, and the most significant genes are HLA-A, HLA-B, and HLA-C, which are involved in antigen processing and presentation of endogenous peptide antigen via the MHC class I via ER pathway, TAP-independent. The log2FC values for HLA-A, HLA-B, and HLA-C genes were higher, with a twofold greater prevalence observed in the ABMR group compared to the TCMR group.

Our study has several limitations. Primarily, the sample size for each group is limited, totaling six samples. Secondly, due to the implementation of for-cause

biopsies, the NOMOA group, designated as the control group, may not be the ideal representation of a control group. Thirdly, the mean duration from surgery to blood collection for individuals in the TCMR group was 15 months, exceeding the commonly recognized 12-month window associated with the occurrence of TCMR. Lastly, the validation of the identified DEGs through Western blot or transgenic mice experiments could not be carried out. Nevertheless, there is a lack of single-cell sequencing studies using PBMCs from kidney transplant recipients, and no literature specifically comparing TCMR can be found. Furthermore, given the existing studies confirming the involvement of the four finally selected genes in renal transplant rejection and corneal rejection, we anticipate that future research will focus on validating the genes discovered in this study. Furthermore, in addition to the four genes selected through STRING analysis, we anticipate that further understanding may be gained from subsequent studies with similar parameters among the genes identified as significant.

In conclusion, we identified significant cell types and DEGs associated with ABMR in PBMCs from KT recipients. In the context of ABMR, *LGALS1* and *ITM2A* in CD8+ Temra T cells, and *CD160* and *HLA-F* in NK T cells, unequivocally play pivotal roles. The findings of this research will help identify transcripts that are suitable for future investigations into the mechanisms of antibody-mediated rejection and non-invasive diagnostic approaches.

5. **References**

1. OPTN/SRTR 2018 Annual Data Report: Introduction. *Am J Transplant*. Jan 2020;20 Suppl s1:11-19. doi:10.1111/ajt.15671

2. Hariharan S, Israni AK, Danovitch G. Long-Term Survival after Kidney Transplantation. *N Engl J Med*. Aug 19 2021;385(8):729-743. doi:10.1056/NEJMra2014530

3. Lentine KL, Smith JM, Hart A, et al. OPTN/SRTR 2020 Annual Data Report: Kidney. *Am J Transplant*. Mar 2022;22 Suppl 2:21-136. doi:10.1111/ajt.16982

4. Loupy A, Haas M, Roufosse C, et al. The Banff 2019 Kidney Meeting Report (I): Updates on and clarification of criteria for T cell- and antibody-mediated rejection. *Am J Transplant*. Sep 2020;20(9):2318-2331. doi:10.1111/ajt.15898

5. Anglicheau D, Suthanthiran M. Noninvasive prediction of organ graft rejection and outcome using gene expression patterns. *Transplantation*. Jul 27 2008;86(2):192-9. doi:10.1097/TP.0b013e31817eef7b

6. Habal MV, Farr M, Restaino S, Chong A. Desensitization in the Era of Precision Medicine: Moving From the Bench to Bedside. *Transplantation*. Aug 2019;103(8):1574-1581. doi:10.1097/TP.0000000000002737

7. Sarwal M, Chua MS, Kambham N, et al. Molecular heterogeneity in acute renal allograft rejection identified by DNA microarray profiling. *N Engl J Med*. Jul 10 2003;349(2):125-38. doi:10.1056/NEJMoa035588

8. Pineda S, Sur S, Sigdel T, et al. Peripheral Blood RNA Sequencing Unravels a Differential Signature of Coding and Noncoding Genes by Types of Kidney Allograft Rejection. *Kidney Int Rep*. Oct 2020;5(10):1706-1721. doi:10.1016/j.ekir.2020.07.023

9. Madill-Thomsen K, Perkowska-Ptasinska A, Bohmig GA, et al. Discrepancy analysis comparing molecular and histology diagnoses in kidney transplant biopsies. *Am J Transplant*. May 2020;20(5):1341-1350. doi:10.1111/ajt.15752

10. Kong F, Ye S, Zhong Z, et al. Single-Cell Transcriptome Analysis of Chronic Antibody-Mediated Rejection After Renal Transplantation. *Front Immunol*. 2021;12:767618. doi:10.3389/fimmu.2021.767618

11. Vegh P, Haniffa M. The impact of single-cell RNA sequencing on understanding the functional organization of the immune system. *Brief Funct Genomics*. Jul 1 2018;17(4):265-272. doi:10.1093/bfgp/ely003

12. Zhang Z, Qin Y, Wang Y, Li S, Hu X. Integrated analysis of cell-specific gene expression in peripheral blood using ISG15 as a marker of rejection in kidney transplantation. *Front Immunol*. 2023;14:1153940. doi:10.3389/fimmu.2023.1153940

13. Hidalgo LG, Sis B, Sellares J, et al. NK cell transcripts and NK cells in kidney biopsies

from patients with donor-specific antibodies: evidence for NK cell involvement in antibody-mediated rejection. *Am J Transplant*. Aug 2010;10(8):1812-22. doi:10.1111/j.1600-6143.2010.03201.x

14. Kildey K, Francis RS, Hultin S, et al. Specialized Roles of Human Natural Killer Cell Subsets in Kidney Transplant Rejection. *Front Immunol*. 2019;10:1877. doi:10.3389/fimmu.2019.01877

15. Amodio G, Cichy J, Conde P, et al. Role of myeloid regulatory cells (MRCs) in maintaining tissue homeostasis and promoting tolerance in autoimmunity, inflammatory disease and transplantation. *Cancer Immunol Immunother*. Apr 2019;68(4):661-672. doi:10.1007/s00262-018-2264-3

16. Jacquemont L, Tilly G, Yap M, et al. Terminally Differentiated Effector Memory CD8(+) T Cells Identify Kidney Transplant Recipients at High Risk of Graft Failure. *J Am Soc Nephrol*. Apr 2020;31(4):876-891. doi:10.1681/ASN.2019080847

17. Yap M, Boeffard F, Clave E, et al. Expansion of highly differentiated cytotoxic terminally differentiated effector memory CD8+ T cells in a subset of clinically stable kidney transplant recipients: a potential marker for late graft dysfunction. *J Am Soc Nephrol*. Aug 2014;25(8):1856-68. doi:10.1681/ASN.2013080848

18. Lai Q, Hu L, Zhang W, Jiang Z, Zeng C, Hu J. Single-Cell RNA sequencing highlights the regulatory role of T cell marker genes Ctla4, Ccl5 and Tcf7 in corneal allograft rejection of mouse model. *Int Immunopharmacol*. Apr 2023;117:109911. doi:10.1016/j.intimp.2023.109911

19. Dooley BJ, Verma A, Ding R, et al. Urinary Cell Transcriptome Profiling and Identification of ITM2A, SLAMF6, and IKZF3 as Biomarkers of Acute Rejection in Human Kidney Allografts. *Transplant Direct*. Aug 2020;6(8):e588. doi:10.1097/TXD.0000000000001035

20. Del Rio ML, Nguyen TH, Tesson L, et al. The impact of CD160 deficiency on alloreactive CD8 T cell responses and allograft rejection. *Transl Res*. Jan 2022;239:103-123. doi:10.1016/j.trsl.2021.08.006

6. Supplementary data

Supplementary Table 1. Cell and subtype cell marker for annotation

Cell type	Cell subtype	Surface markers
CD4+ T cell		CD3D, CD3G, CD4
	Naïve	CCR7, SELL+++
	Central memory (CM)	CCR7, SELL+
	Tfh	LAG3, MAF, IGFL2+++
	Th1	TBX21, IFNGR1+, CXCR3+
	Th2	GATA3
	Th9	IL4, IL10++
	Th17	CCR6+, KLRB1++
	Th22	CCR10++
	Treg	FOXP3++
CD8+ T cell		CD3D, CD3G, CD8A, CD8B
	Naïve	CCR7, SELL+++, IL7R+
	Central memory	CCR7, SELL+, IL7R+++, CD27, CD28+
	Effector memory	IL7R+, KLRG1++, PRF1, GZMB++
	Effector	IL7R-, CCL4, CCL5, PRF1, GZMB++
	Terminally differentiated effector memory (Temra)	ASCL2, CX3CR1+, GZMH+, CD27, CD28-
	gd-like	TRGC1, TRDC ++
	Tc17	KLRB1, ZBTB16++
	Proliferating	MKI67, PCNA++
	HBB+	HBB+
B cell		CD19, CD24, CD40, CD72
	Naïve B cell	IL4R, IGHD
	Memory B cell	CD19, MS4A1
	Plasma cell	IGHG1, MZB1, SDC1
NK T Cell		CD3E, CD3G, CD3D, NCAM1, KLRD1, FCGR3A
NK cell		CD3-, NCAM1, KLRD1, FCGR3A
	CD56 Bright NK cell	NCAM1
	CD56 dim NK cell	FCGR3A
Monocyte		CD14, FCGR3A
	Classical	CD14

	Intermediate	CD14, FCGR3A
	Nonclassical	FCGR3A

Supplementary Table 2. Pathologic findings according to the Revised Banff 2019 classification

Banff score	NOMOA1	NOMOA2	TCMR1	TCMR2	ABMR1	ABMR2
g	0	0	0	0	2	1
ptc	0	0	2	0	3	2
v	0	0	0	0	0	0
cg	0	0	0	0	0	0
cv	1	1	3	1	3	1
ptcml	0	0	0	0	0	0
C4d>0	0	60%	0	1%	0	5%
i	0	0	3	3	0	0
t	0	0	2	3	1	1
ci	1	0	1	1	1	1
ct	1	1	2	1	1	1
ti	0	0	3	3	0	1
mm	1	0	2	1	0	1
ah	0	1	2	1	1	2
i-IFTA	1	0	2	3	0	1
t-IFTA	0	0	2	3	1	0
aah	0	0	1	0	0	1
pvl	0	0	0	0	0	0

Supplementary Table 3. Proportions of different cell types

Cell type	NOMOA group (%) n=9501	TCMR group (%) n=11766	ABMR group (%) n=11918
CD4+ T cell	3492 (36.8)	4019 (34.2)	3613 (30.3)
CD8+ T cell	2297 (24.2)	3292 (28.0)	3261 (27.4)

T cell	751 (7.9)	758 (6.4)	370 (3.1)
NKT cell	636 (6.7)	1034 (8.8)	903 (7.6)
NK cell	850 (8.9)	1049 (8.9)	846 (7.1)
B cell	170 (1.8)	785 (6.7)	970 (8.1)
Monocyte	1050 (11.1)	634 (5.4)	1575 (13.2)
DC	148 (1.6)	152 (1.3)	141 (1.2)
Platelet	107 (1.1)	43 (0.4)	239 (2.0)

Supplementary Table 4. Proportions of different subset cell types

Subset cell type	NOMOA group (%)	TCMR group (%)	TCMR/ NOMOA (%)	ABMR group (%)	ABMR/ NOMOA (%)
CD8+	2704	3712		3513	
Naïve T cell	371 (13.7)	447 (12.0)	87.6	907 (25.8)	188.3
CM T cell	641 (12.6)	620 (16.7)	132.5	387 (11.0)	87.3
EM T cell	467 (17.3)	625 (16.8)	97.1	485 (13.8)	79.8
Effector T cell	390 (14.4)	442 (11.9)	82.6	238 (6.8)	47.2
Temra T cell	598 (22.1)	886 (23.9)	108.1	1114 (31.7)	143.4
gd like T cell	51 (1.9)	148 (4.0)	210.5	62 (1.8)	94.7
Tc17 cell	104 (3.8)	182 (4.9)	128.9	143 (4.1)	107.9
Proliferating T cell	55 (2.0)	39 (1.1)	55.0	42 (1.2)	60.0
HBB+ T cell	327 (12.1	323 (8.7)	71.9	135 (3.8)	31.4
CD4+	3570	4088		3616	
CM T cell	353 (9.9)	361 (8.8)	88.9	310 (8.6)	86.9
gd like T cell	9 (0.3)	6 (0.1)	33.3	5 (0.1)	33.3
Naïve T cell	1502 (42.1)	1454 (35.6)	84.6	1614 (44.6)	105.9
T reg cell	101 (2.8)	193 (4.7)	167.9	137 (3.8)	135.7
Tfh cell	44 (1.2)	28 (0.7)	70	36 (1.0)	83.3
Th1 cell	350 (9.8)	606 (14.8)	107.2	499 (13.8)	140.8
Th17 cell	947 26.5)	1090 (26.7)	124.2	779 (21.5)	81.1
Th22 cell	264(7.4)	350 (8.6)	132.3	236 (6.5)	87.8
NK	1486	2083		1749	

CD56 bright NK cell	106 (7.1)	150 (7.2)	101.4	51 (2.9)	40.8
CD56 dim NK cell	1017 (68.4)	1388 (66.7)	97.5	1077 (61.6)	90.1
NK T cell	363 (24.4)	545 (26.2)	107.4	621 (35.5)	145.5
Myeloid	1230	843		1791	
IL1β+ monocyte	87 (7.1)	143 (17.0)	239.4	106 (5.9)	83.1
Classical monocyte	524 (42.6)	222 (26.3)	61.7	816 (45.6)	107
Intermediate monocyte	188 (15.3)	51 (6.0)	39.2	284 (15.9)	103.9
Non-classical monocyte	122 (9.9)	123 (14.6)	147.5	170 (9.5)	96.0
pDC	54 (4.4)	51 (6.0)	136.4	27 (1.5)	34.1
cDC1	18 (1.5)	41 (4.9)	326.7	13 (0.7)	46.7
cDC2	105 (8.5)	86 (10.2)	120	120 (6.7)	78.8
Platelet	13 (1.1)	0 (0.0)	0	90 (5.0)	454.5
Doublet	119 (9.7	126 (14.9)	162.0	165 (9.2)	94.8
B cell	138	721		895	
Memory B cell	56 (40.6)	75 (10.4)	25.6	142 (15.9)	202.1
Naïve B cell	80 (58.0)	623 (86.4)	149.0	730 (81.6)	727.4
Plasma cell	2 (1.4)	23 (3.2)	228.6	23 (2.6)	916.8

Supplementary Table 5. Meaningful DEGs associated with ABMR in each subtype cells

Cell	Meaningful DEGs
CD8+ Temra T cell	*ACTG1, ACTR3, ANXA1, CD2, CRIP1, GZMA, HLA-DPA1, HLA-DQA1, HLA-DRB1, IFITM2, ITGB1, ITM2A, KLRD1, LGALS1, S100A11, STAT1, TRAC, TRGC2, VIM, ZNF683*
NK T cell	*ACTG1, ACTR3, ANXA1, CD160, CD2, CD3D, CD3G, CRIP1, CX3CR1, HCST, HLA-DPA1, HLA-DPB1, HLA-DQA1, HLA-DRB1, HLA-F, IL32, KEGG, KLRB1, KLRC3, KLRD1, KLRD1, NCR3, NCR3, PRELID1, STAT1, TRDC, TRGC1, VIM*
IL1β+ monocytes	*ADGRE5, AKAP13, ALOX5, AP3B1, APP, B2M, BSG, BST1, CASP8, CCDC88B, CD14, CD36, CD4, CD46, CD84, CSF3R, CTSD, CTSH, CTSS, CYBA, CYBB, FOS, FPR1, HLA-A, HLA-B, HLA-C, HLA-DQB1, HLA-DRB1, HLA-E, HLA-F, ICAM3, ITGA5, ITGAM, JAML, LILRB3,*

MPEG1, NAIP, NCF1, NCKAP1L, PNN, POU2F2, PPBP, PTAFR, PTPRC, RIPOR2, S100A12, S100A8, SIRPA, SLC11A1, TCIRG1, TNFRSF1B, TNFSF10, TRIM38, TRIM56, TXNIP, VCAN, VCL, CANX

Supplementary Figure 1. Quality control and filtering

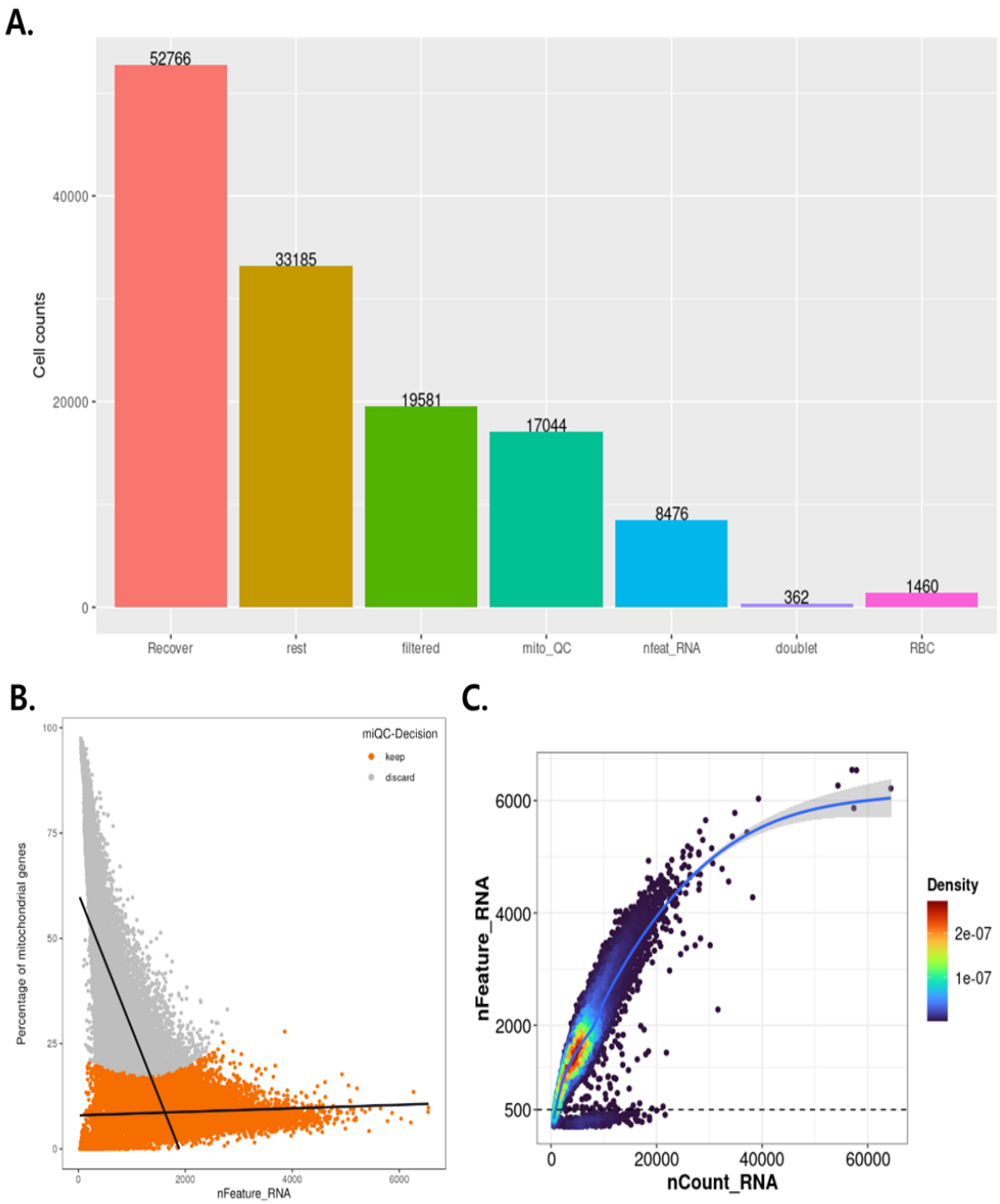

Supplementary Figure 2. T cell subset markers and quality control

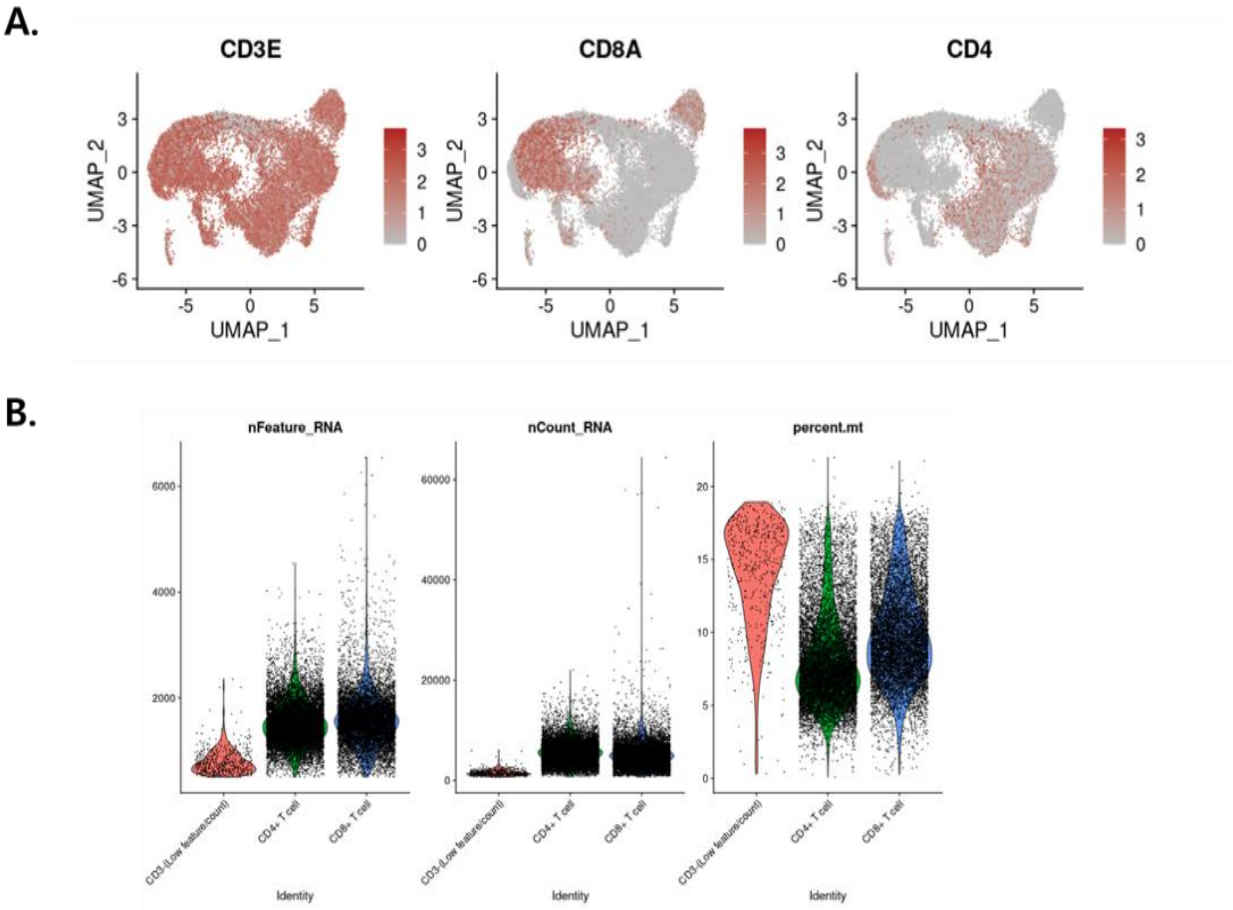

Supplementary Figure 3. Second annotation of CD4+ T cells, B cells, and myeloid cells

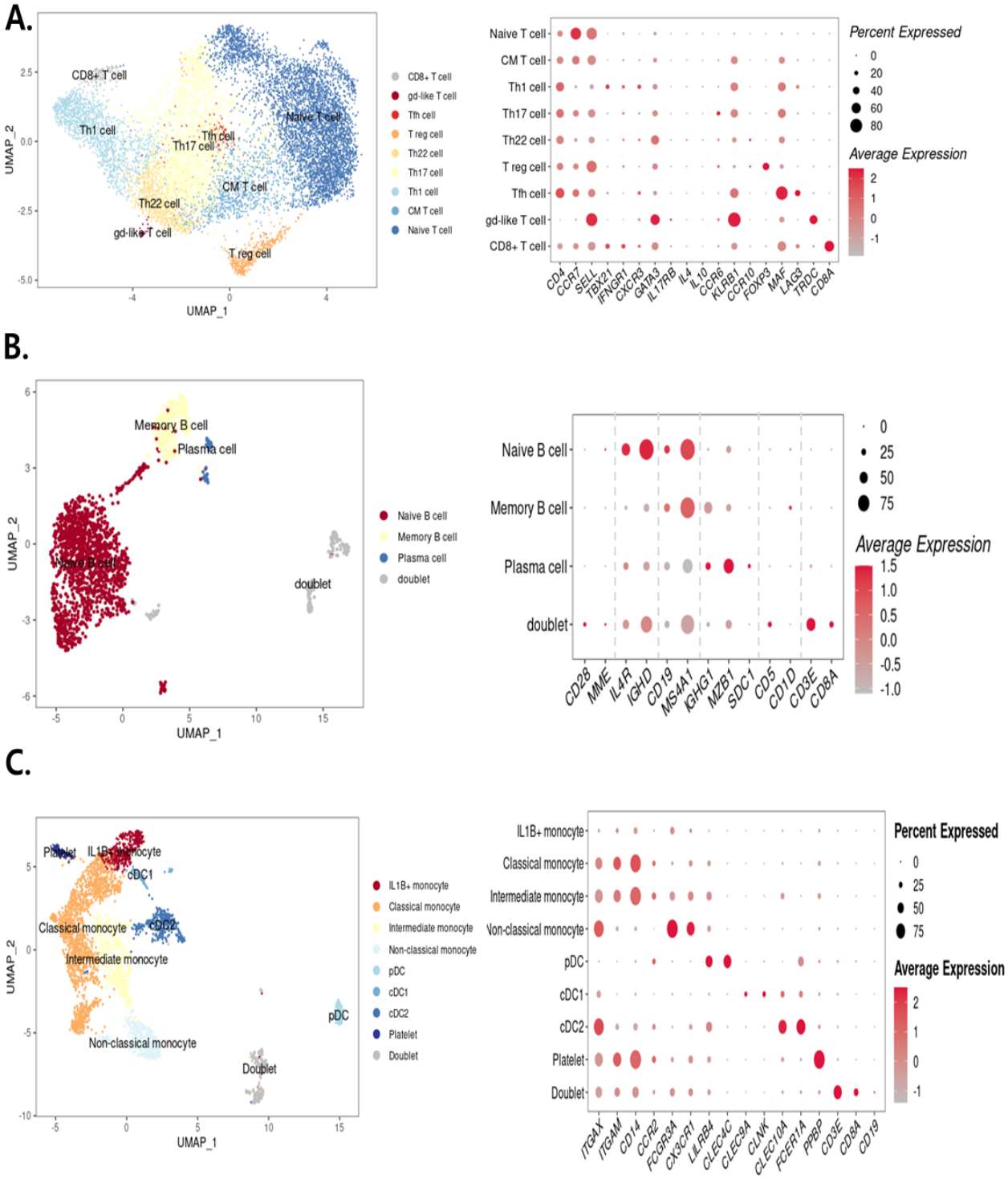

Supplementary Figure 4. ABMR-specific DEGs and meaningful DEGs in IL1β+ monocytes

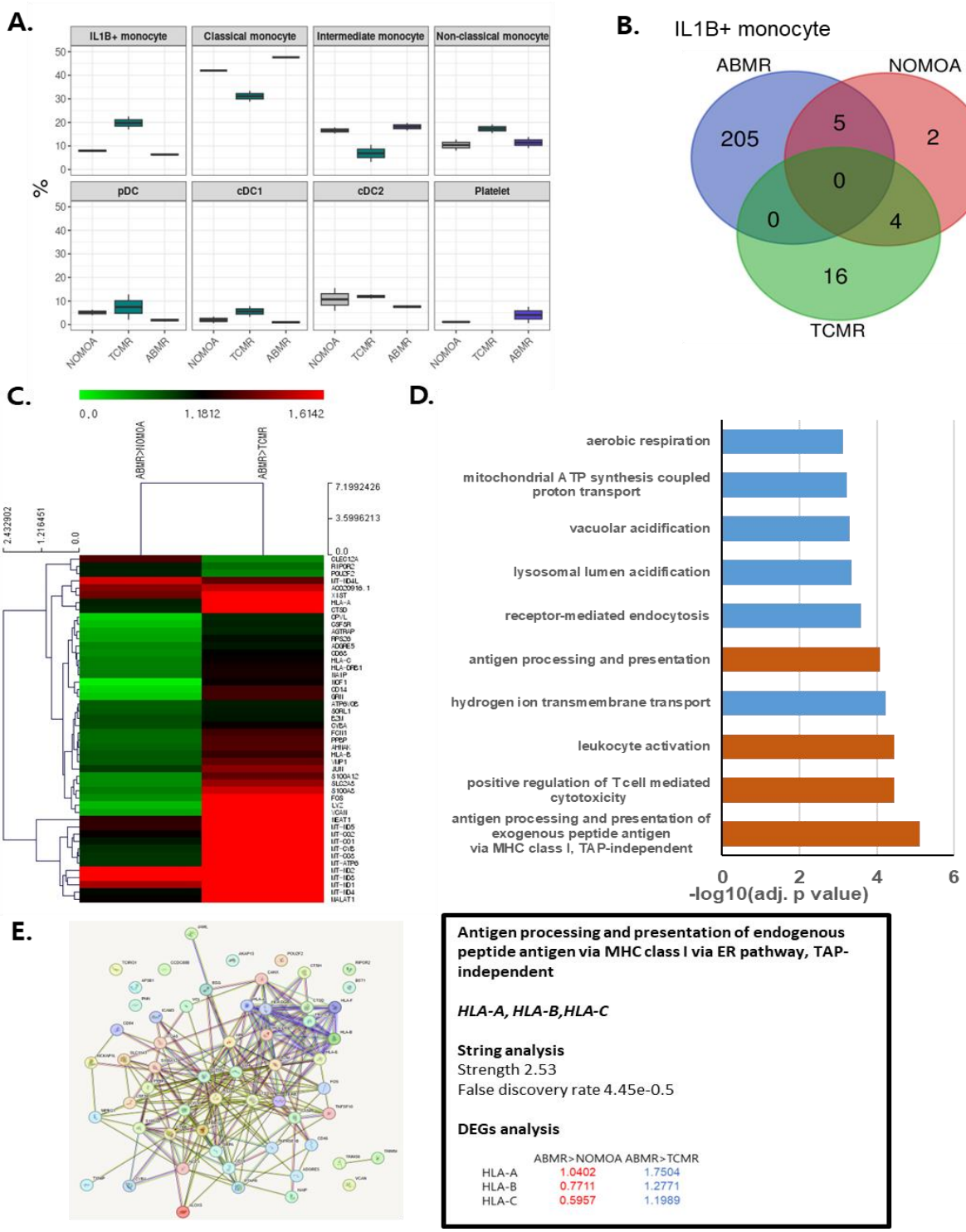

국문요약(Korean abstract)

서론

말초 혈액 기반 유전자 발현 패턴을 이용한 면역 경로 분석은 신장 이식 수혜자의 거부 반응 메커니즘을 찾는 데 사용되었습니다. 특히, 단일세포 시퀀싱은 특정 세포에서 유전자 발현을 확인함으로써 보다 구체적인 연구를 가능하게 했다. 우리는 신장 이식 후 차등 발현 유전자(Differential Expression Genes; DEGs) 관련 항체 매개 거부반응과 T 세포 매개 거부반응을 발견하는 것을 목표로 했습니다.

연구방법

신장이식 수혜자 6명을 대상으로 원인생검을 실시하였고, 2019 Banff 기준에 따라 주요 이상이 없음(NOMOA), T세포 매개 거부반응 (TCMR), 항체 매개 거부반응 (ABMR)의 3개 그룹으로 나누었습니다. 이들 환자의 말초 혈액 단핵 세포를 사용하여 포괄적인 단일 세포 서열 분석을 수행했습니다. 그리고 Gene Ontology biological process 분석을 이용하여 유전자의 기능을 확인하였습니다.

결과

총 52766개의 세포 중 퀄리티가 떨어지는 세포들을 제외하고 33185개의 세포를 분석하였습니다. CD8+ Temra T cell 및 NK T cell이 ABMR 그룹에서 많이 분포하였습니다. CD8+ Temra T cell에서 ABMR specific gene은 36개였고 이중 면역반응 및 염증반응에 관여한 차등 발현 유전자는 20개를 확인하였습니다. 20개의 유전자를 이용한 String analysis 결과 가장 관련이 깊은 유전자는 *LGAS1*과 *ITM2A*였고 plasma cell differentiation에 관여하였습니다. NK T cell에서 ABMR specific gene은 48개였으며 이중 Geone Ontology biological pathway에서 의미있는 기능을 가진 유전자는 28개였습니다. 이중 string analysis에서 가장 관련이 깊은 유전자는 *CD160*과 *HLA-F*로 positive regulation of NK cell degranulation에 관여하는 것으로 확인되었습니다. TCMR 그룹에서는 최종 의미 있는 세포와 DEGs는 확인되지 않았습니다.

결론

우리는 신장 이식 환자의 PBMC 분포를 조사하고 각 세포에서 DEGs를 확인했습니다. 항체 매개 거부반응에서 CD8+ Temra T cell의 *LGALS1*과 *ITM2A*가 NK T cell의 *CD160*과 *HLA-F*가 중요한 기능을 하는 것으로 보입니다. 본 연구 결과는 추후 항체 매개 거부반응의 기전과 비침습적 진단에 이용될 수 있는 전사체를 찾는데 도움이 될 것입니다.